Harvard Research and Publications International

September 30, 2021 Vol. 16 No. 2 ISSN: 0081 – 3998

JOURNAL OF AFRICAN SUSTAINABLE DEVELOPMENT

FACILE CYTOTOXIC AND APOPTOTIC EFFECTS OF DOXORUBICIN ENCAPSULATED $CACO_3$-NANOPARTICLES ON MCF-7 (BREAST CANCER) CELL-LINE

HAMIDU AHMED[1, 3]; ALHAJI ZUBAIRJAJI[2]

[1]Laboratory of Molecular Biomedicine, Institute of Bioscience, Universiti Putra Malaysia, Serdang, Selangor Malaysia [2]Department of Preclinical Science, Faculty of Veterinary Medicine, Universiti Putra Malaysia, Serdang, Selangor, Malaysia. [3]Department of Material Science and Nanotechnology, Federal Polytechnic Mubi, Adamawa State, Nigeria

Abstract

Breast cancer is the most prevalent malignant disease of women globally. Aragonite calcium carbonate nanoparticles (Ar-CC-

Keywords:
Apoptosis, Cytotoxicity, Cancer, Drug Delivery, MCF-7 Cell Line

INTRODUCTION

In spite multimodal system in the treatment of breast cancer using chemotherapeutics, its clinical utility is hampered by several factors such as toxicity, the measure of effectiveness and safety of chemotherapy (1). Nanomedicine has recently offered a potential new method for treating cancer, through their tunable pharmacokinetics properties, larger surface area, enhanced solubility of the drug, and control release flexibility (2). Their ability to combine fewer toxic phytochemicals with target-specific nanoparticles is advantages and offers a new feature to the standard approaches. Doxorubicin (DOX) is commonly used as a chemotherapeutic agent, either alone

NPs) are a renowned Nano carrier for anticancer delivery. The study aimed at evaluating the cytotoxic and apoptotic effects of Doxorubicin-Aragonite Calcium Carbonate Nanoparticles (DOX-Ar-CC-NPs) on MCF-7 cancer cells and to elucidate its mechanism of action. Hence, giving an insight into how Ar-CC-NPs influence efficient drug target delivery and improve therapeutic index. Ar-CC-NPs was synthesized using novel biomolecules from cheaply available sea water cockleshell and characterized for particle geometry using electron microscopy. The cytotoxic effect of DOX-Ar-CC-NPs was determined using superoxide dismutase analysis for cell membrane integrity, and flow cytometry, fluorescent imaging, and electron microscopy were used for apoptotic evaluation. Dose-dependent cell viability was recorded in DOX-Ar-CC-NPs and DOX treated MCF-7 cells. The DOX-Ar-CC-NPs had a significant inhibitory effect on cell viability when compared with DOX alone ($p<0.05$). Cellular apoptosis, oxidative stress markers and cellular uptake evaluation showed a similar trend. The results clearly showed that DOX-Ar-CC-NPs induced necrosis through endocytosis. Conversely, treatment with DOX-Ar-CC-NPs significantly decreased the elevated level of superoxide dismutase 2 compared to untreated MCF-7 cells. Furthermore, membrane blebbing's and apoptotic bodies were observed on ultra-structurally, when treated with DOX-Ar-CC-NPs, it reveals that breast cancer cells treated with DOX-Ar-CC-NPs, are capable of inducing apoptosis. This study revealed the ability of Ar-CC-NPs to optimize the ability of DOX to induce apoptosis in MCF-7 cells thus, emphasizing the high potency of Ar-CC-NPs understudy in drug delivery.

Or in combination with other anti-tumor agents to treat a variety of carcinomas osteosarcomas and Hodgkin's and non-Hodgkin's lymphomas (3). Nevertheless, clinical usage of DOX is associated with congestive heart failure and cardiomyopathy, weight loss and mucositis, which raised concern among physician (4).

One more major clinical setback in chemotherapy against breast cancer is the enhancement of drug resistance (5).Thus, there is an imperative condition for improving the cytotoxic as well as apoptotic effects of doxorubicin conjugated Aragonite $CaCO_3$ nanoparticles (DOX-Ar-CC-NPs) on MCF-7 cells and limiting undesirable adverse side effects (4). With the expectation to do away with the impediments of the typical chemotherapy, a several numbers of drug delivery approaches with nanotechnology have been revealed in the earlier period (6,7). Additionally, a drug delivery method could be aimed to release the drug act in response to a particular stimulus such as pH temperature, ultrasound intensity and magnetism (6). Amongst these stimuli pH-sensitive, delivery system is considered as the most common therapeutic strategy for the treatment of cancer, owing to the substantial pH variations existing between characteristic physiological environment in addition to acidic microenvironment of lysosomes otherwise tumor (8,9). Typically, aragonite $CaCO_3$ nanoparticles (Ar-CC-NPs) delivers DOX into cancer cells by endocytosis (6,7,10) As a result, the efflux pumps localized protein in the cytoplasmic membrane as a means to overcome drug resistance (9).

One of the crucial features of DOX-Ar-CC-NPs carriers is their lack of intrinsic properties and features (11). These suggest that the cytotoxicity of DOX loaded into Ar--CCNPs can be ascribed to different factor but not exclusive mechanisms. The DOX-Ar-CC-NPs analysis using ultrastructural TEM, SEM, cellular uptake, and flow cytometry analysis of the Ar-CC-NPs-treated cells with DOX, might provide vital clues in this regard.

The study evaluated the cytotoxic and apoptotic effects of DOX-Ar-CC-NPs on MCF-7 cell lines, including its molecular mechanism and oxidative stress levels. This might give an insight into the agent influences on chemo-resistivity and drug target delivery, towards limiting undesirable side effects, In addition, the nanoparticle complex could increase the biodistribution of the drug in the target sites avoiding the normal cells (12–15) It also aimed at revealing the ability of DOX-Ar-CC-NPs to induce apoptosis in MCF-7 cells and further indicate the potential of Ar-CC-NPs in drug delivery.

Materials and Methods

Material and chemical reagents.

Human MCF-7 Cell lines (ATCC ® CRL-11372™) were acquired from the American Type culture collection (ATCC, USA). MCF-7 cells were grown in Dulbecco's modified eagle's medium (DMEM) (Nacal Tesque, Kyoto, Japan), which was supplemented with 10% Fetal Bovine Serum (FBS) and 1% penicillin-streptomycin (PAA, Austria). Less than 10 passage cells cultured were used. However, all other chemicals used were of analytical grade from different commercial suppliers.

Synthesis of the Ar-CC-NPs

Synthesis of Ar-CC-NPs was initiated using 5 g cockle shell micron-sized powders as previously described by Danmaigoro *et al.,* (2017). Briefly, the micron sized powder was stirred at 1000 rpm with deionized water and surfactant (BS-12), for 120 minutes and filtered and packaged. The sediment was dried in an oven for 72 hours and stored for further analysis.

Encapsulation of DOX-Ar-CC-NPs

The encapsulation of DOX-Ar-CC-NPs was done as early described (6,10) with the higher encapsulated efficiency formulation used for all the analysis.

Cell Culture

MCF-7 cells were passaged in high-glucose DMEM supplemented with 10% FBS, penicillin (100 µg/mL) and Streptomycin (100 µg/mL), in 5% CO_2 incubator at 37^{o} C (Thermo Fisher Scientific, USA). The cells were further sub-cultured to attain a confluence range of 80 to 90%. The confluence of MCF-7 cells was detached with 0.5 mL trypsin-EDTA solution within 3-5 minutes, and washed immediately with fresh growth medium to prevent the toxic effect of trypsin on the cells. Further, 100 µL (1×10^4) cells suspensions were seeded in 96-well plates and finally incubated for 24 hours.

Apoptosis evaluation assay

The apoptosis evaluation assay of DOX and DOX-Ar-CC-NPs was conducted

using fluorescence microscopy. The medium of seeded MCF-7 (5×10^5) cells/well in 6-well plates, after 48 hours incubation was discarded and replaced with new fresh media with the cells treated with DOX and DOX-Ar-CC-NPs of an equivalent concentration with DOX (0.5µg/mL) for 48 and 72 hours at 37° C. However, before the end of incubation, Acridine Orange (AO) and Propidium Iodide (PI) double staining was added to control, apoptosis and necrosis in accordance to the standard protocol of Plemel *et al.,* (2017). Approximately, 200 µL of the cells were trypsinized and transferred to 15 mL tube. Then, adherent cells were resuspended in a cool phosphate buffered saline (PBS) and attached to the microscope slides thus, viewed under a fluorescence microscope (Nikon ELIPSE Ti S, Japan).

Cellular uptake Assay

The cellular uptake of DOX and DOX-Ar-CC-NPs were evaluated using fluorescence microscopy. The seeded MCF-7 (5×10^5 cells/well) on 22mm glass coverslips that were placed in 6-well plates. After 24 hours of incubation, the media were discarded and replaced with fresh complete growth medium, including 0.5 µg/mL of DOX or DOX-Ar-CC-NPs (with equivalent concentration) for 24, 48 and 72 hours at 37° C. Thirty (30) minutes before each incubation period, Lyso-ID green dye was added to the culture medium to label the endosomes and lysosomes. Consequently, the media was aspirated, with the cells were rinsed two times with PBS. Then the cells were fixed with 4% paraformaldehyde for 30 minutes. After washing with PBS, the fixed cells were mounted onto microscope slides. The fluorescent distribution was then visualized under a fluorescent microscope (Nikon ECLIPSE Ti S, Japan).

Morphological Examination

Light Microscopy

MCF-7 cells were passaged in 6-well plates at 5×10^5 cells/well in 1.5 mL of a fresh complete growth medium, incubated for 24 hours and treated with 0.5µg/ml of free DOX and DOX-Ar-CC-NPs (with an equivalent concentration of free DOX) for 48 hours at 37° C in 5% CO_2 incubator. Control cells were treated with fresh media. After the exposure was completed, the used media was discarded and rinsed twice with PBS. After

that, the cells were attached in 4% paraformaldehyde for half an hour. Cellular morphology was immediately examined, and images were captured using an inverted light microscope (Olympus, Japan).

Transmission Electron Microscopy

MCF-7 cells were passaged in six well plates at 5×10^5 cells/well in 1.5 mL of the growth medium incubated for 24 hours then treated with Doxorubicin and DOX-Ar-CC-NPs (with corresponding of DOX) for 48 hours. The control cells were treated with growth medium alone. As soon as 48 hours of incubation, the cells were rinsed with PBS then harvested. As a result, the cells were attached with 4% glutaraldehyde for 24 hours at 4 ^{o}C and post-attached in 1% osmium tetra-oxide for 4 ^{o}C for 2 hours. After fixing, cells were rinsed in triplicate with 0.1 M sodium cacodylate buffer followed by dehydration in ascending grades of acetone (35%, 50%, 75%, 95%, and 100%). At this point, the cells were passed through with resin and fixed with 100% resin in beam capsule, and then left to polymerize at the rate of 60 ^{o}C for 48 hours. Afterwards, the allotted area was censored into ultrathin sections with a microtome, and positioned onto copper grids and stained with uranyl acetate and citrate. The stained samples were observed via High Resolution Transmission Microscope (HT-TEM) (Hitachi H-7100., Japan), operated at150kV.

Scanning Electron Microscopy

The IC_{50} concentration dose of DOX and DOX-Ar-CC-NPs were used to trigger cell apoptosis in MCF- 7 cells. First, the cells were co-passaged with fresh growth media. After 48 hours, the cells were trypsinized, centrifuged at 1500 rpm for 10 minutes and the pellets were fixed in 4% glutaraldehyde for 24 hours at 4 ^{0}C. Second, the attached cells were rinsed in 3 times with 0.1 M sodium cacodylate buffer for 10 minutes each and post-attached in 1% osmium tetra-oxide 2 hours at 4 ^{0}C. After fixation, the cells were dehydrated in ascending order grades of acetone (35%, 50%, 75%, and 100%) and carried to the critical point of exposure to air using critical point-drier (CPD 030, Bal-TEC, Switzerland) for about 30 min. For scanning Electron Microscope (SEM) analysis, MCF-7 Cells were dispensed onto a sub covered with an adhesive conductive carbon tab and sputter-

coated in gold by using the SEM coating unit (E5100 Polaron, UK). The coated samples were observed with SEM (JOEL 6400, Japan).

Superoxide dismutase (SOD) activity

The superoxide dismutase activity was measured using a commercial colorimetric assay kit, OxiSelect SOD Activity (Cell Biolabs, Inc., San Diego, CA). In brief, after the treatments of MCF-7 cells with DOX and DOX-Ar-CC-NPs the cells were rinsed with ice-cold PBS and incubated in ice-cold lysis buffer for 10 minutes. Following incubation, cells were centrifuged at 12000g for 10 minutes to pellet the cells 10 µL of supernatant was collected and transferred to 96-well plates. At this point, 10 µL of 10 X assay buffer and 70 µL of deionized water was supplemented to the supernatant. As a final point, 10 µL 1X Xanthine Oxidase Solution was added to each well, and the absorbance was read immediately at 490 nm using spectrophotometer machine.

Determination of Apoptosis by Annexin FITC-V/Propidium Iodide staining

The investigation was carried out according to the manufacturer's instructions (BD Bioscience, USA) with slight modifications. For cellular uptake, cells were passaged in 6-well plates at 1.5 x 10^5 cells/well. The cells were then treated with DOX and DOX-Ar-CC-NPs (0.5 µg/mL) and incubated with 5 mL of complete growth passaged media for 24 hours. Once the incubation is done, the floating cells were discarded, and the adhesive cells were trypsinized to separate the cells. The detached cells were counted and a volume of media containing 1 x 10^5 cells (both death and viable cells) was centrifuged at 1300 x g to acquire a pellet. Next, MCF7 cells were suspended with 100 µL of 1 x assay buffer and 5 µL of Annexin-V fluorescent isothiocyanate (FITC) followed by supplementation of PI solution (5 µL). The samples were gently mixed. After 10 minutes of incubation at room temperature in the dark, 400 µL of 1 x assay buffer and 10 µL of PI (0.5 µg/Ml) were added, and the samples were analyzed at the appointed time by FACSCalibur flow cytometer (Becton Dickinson, CA, USA). For each sample, 10000 measures were collected, and the results were analysed by FlowJo software.

Statistical Analysis

The collected data were analyzed using IBM SPSS software (version 25, USA), to generate descriptive and inferential statistics. For descriptive analysis, the distribution and spread of data were determined mean $\pm$ standard deviation. For inferential analysis, one way analysis of variance. (ANOVA) and Duncan's multiple range test (MRT-a post hoc test) were employed to validate whether there were any statistically significant differences between the test sets. The level of significance was set at $p<0.05$. All experiments were carry-out in triplicate.

Results

Morphological Evaluation of Acridine orange and Propidium Iodide double staining of treated MCF-7 cells

The purpose of using AO/PI double staining fluorescent of MCF-7 method was to morphologically evaluate viable cells, apoptotic and dead cells. The MCF-7 micrographs displayed homogeneous green cells with rounded nuclei (figure. 1A at 48 hours and 1–D after 72 hours). Thus confirms the presence of viable cells since AO stain is impermeable within the viable cell membrane. This confirms the presence of viable cells, since AO was impermeable to viable cells thus observed as greenish discolouration. They are unlike the cells treated with DOX and DOX–Ar-CC-NPs, which revealed mixture of apoptotic cells and viable cells (Figure1B 48 hours, 1C at-72 hours 1E,1F). The apoptotic cells in the early stage have their cell shrinkage with marked granular death cells staining asymmetrically within the cells. Apoptosis aided the evaluation of chromatin condensation (CC) in the nucleus which is associated with early apoptotic nuclei, while the red color was associated with late apoptotic nuclei (AB) and dead cells (DC). The transition to red colour confirmed the increased acidification in the nucleus during apoptosis. The necrotic cells have markedly round and stained with a mixture of orange and red colors. The percentage of apoptotic cells was higher in 72 hours micrographs of the cells. Thus this indicated that < 3 % of necrotic cells were observed upon DOX-Ar-CC-NPs exposure to MCF-7 cells after 48 hours of exposure. The findings in the AO/PI DOX and DOX-Ar-CC-NPs treated cells confirm the induction of

apoptosis of MCF-7 cells, which subsequently led to cell death as depicted in figures1.

Fluorescence Microscopy of (A) DOX alone and (B) DOX-Ar-CC-N Ps

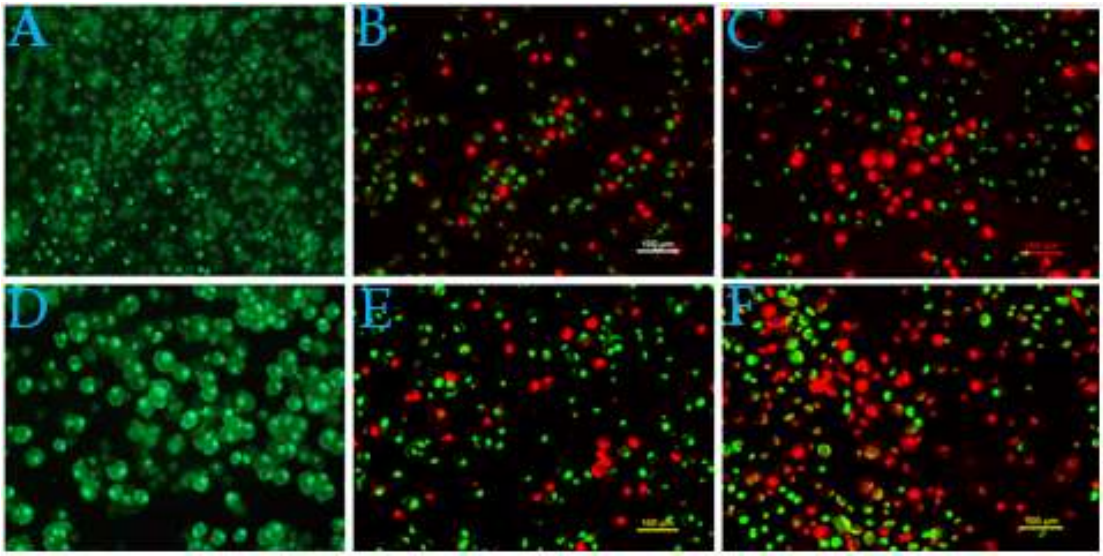

Fig.1: Fluorescent microscopy image of MCF-7 cells stained with Acridine orange (AO/PI) and treated with DOX and DOX-Nanoparticles for 48 hrs. (A) Control (B) treated DOX Green color indicates viable cancer cells and red color indicates apoptotic cells (c) DOX-NPs and for 72 hrs. (D) Control (E) DOX (f) DOX-NPs Magnification × 20, scale bar 100 μm.

Cellular Uptake of DOX and DOX-Ar-CC-NPs

The cellular uptake of MCF-7 cells with DOX-Ar-CC-NPs are shown in figure 2. After 24 hours with DOX-Ar-CC-NPs treatment, weak red fluorescence signals were detected within the cell cytoplasm. However, after 72 hours, a bright red fluorescence was observed in the nucleus, implying the release of DOX from DOX-Ar-CC-NPs and endocytosis-mediated cellular internalization. Although, the cells treated with DOX disclosed a weak red fluorescence in the nucleus after 24 hours. In addition, the red fluorescence increase over time (between 24, to 48 hours). Consequently, for DOX alone, the cells displayed an uneven distribution of red fluorescence throughout the nucleus and cytoplasm with a weaker red fluorescence from DOX which appeared in the nucleus, whereas the cytoplasm displayed a weaker red fluorescence. This clearly shows a direct contact of DOX to the nucleus of

the MCF-7 cells. The incubation time was positively related to cell uptake intensities of both DOX and DOX-Ar-CC-NPs (Figure 2), suggesting that prolonging incubation time may result in more particles entering the cells. Therefore, nanoparticles, based on the DOX-Ar-CC-NPs could help induce apoptosis in MCF-7 cells. This indicates the high potency of the Ar-CC-NPs understudy in drug delivery.

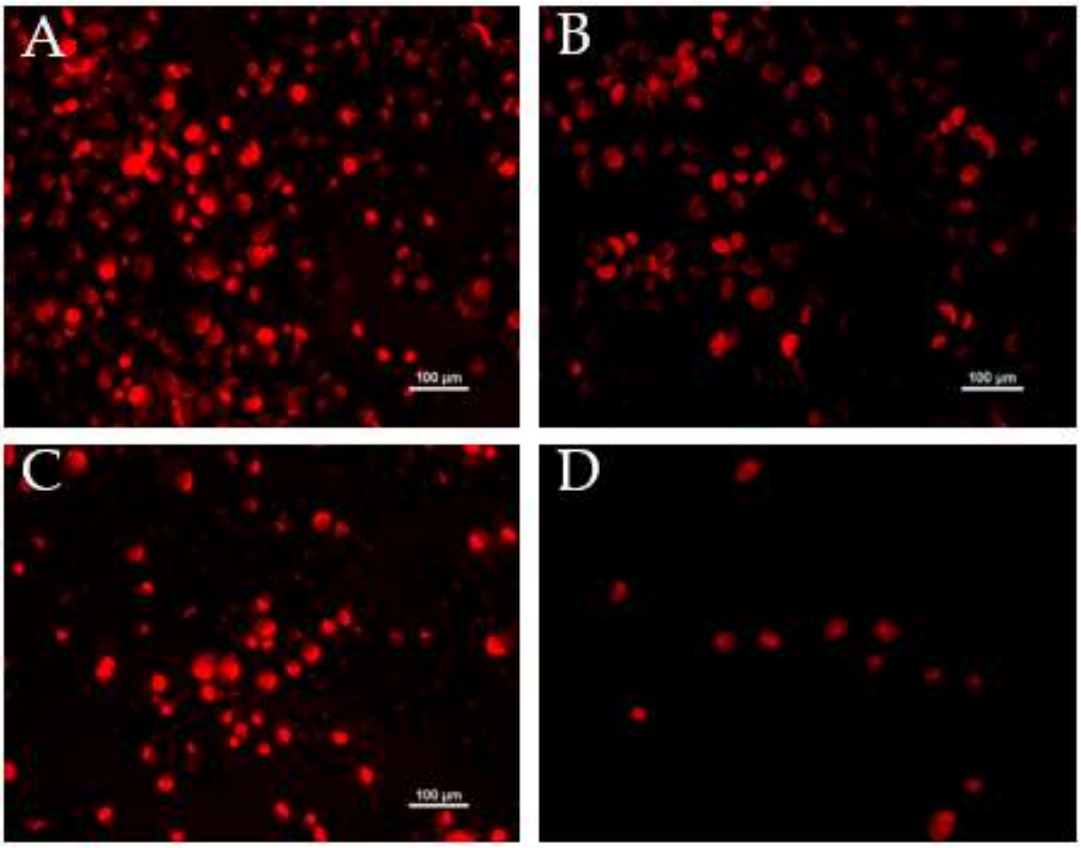

Figure 2. Cellular uptake of Ar-CC-NPs and DOX-Ar-CC-NPs by MCF-7 cells at 48 and 72 hours (magnification x 100). Note: Red dots represent DOX.

An adherent growth and regular polygon cell shapes, with identical few round cells, were observed with MCF-7 in the control group and treated with Ar-CC-NPs (Figure 3A and 3B). In the same way, the number of cells treated with DOX alone as well as DOX-Ar-CC-NPs decreased markedly when compared to the control group. Furthermore, noticeable morphological modifications, such as cells shrinkage, rounding and membrane blebbing's were identified in the cells treated with DOX alone as well as DOX-Ar-CC-NPs after 48 hours, (Figure 3 C to D). As cells shrink,

they detached from neighboring cells and lost contact with adjacent cells. The cells appeared floating in the culture medium and adopted a more rounded morphology. The aggregated Ar-CC-NPs (many small dots) could be examined within or on the surface of the cells. (Figure 3 D). The distinct cells figure decreased as well as morphological alterations demonstrated that DOX-Ar-CC-NPs could release DOX alone and cause apoptosis on MCF-7 cells.

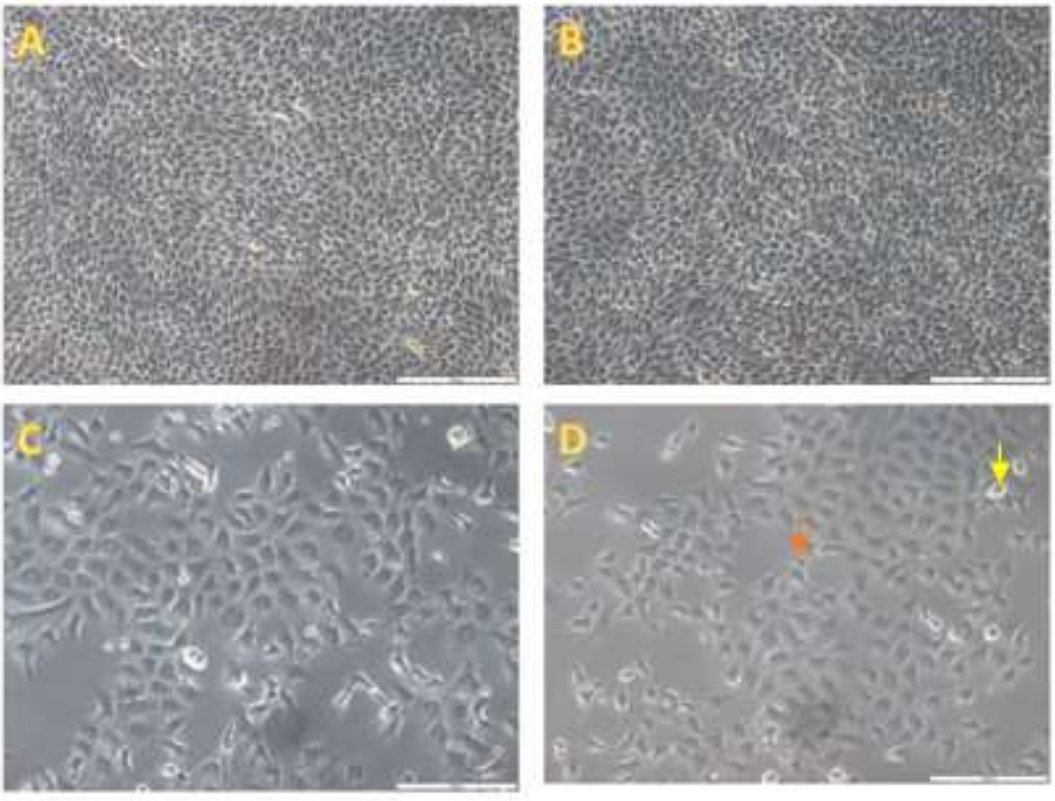

Figure 3: Inverted light microscopy descriptions of MCF-7 cells treated with DOX and DOX-Ar-CC-NPs for72 hours (A) Control Cells (untreated), (B) Cells treated with free NPs, (C) cells treated with DOX, and (D) Cells treated with DOX-NPs, Red arrows indicate cell shrinkage with detachment; yellow arrows indicate DOX-Ar-CC-NPs coacervates (x100)

Ultrastructural Observation of MCF-7 cells using SEM

The control cells reveal typical morphological structures of cancer cells, with numerous lamellipodia and microvilli on the surface (Figure 4A and B) on the evaluation of the surface morphology using SEM. The treatment

groups in Figure 4 (C to F) showed morphological modifications of lamellipodia and microvilli. Furthermore, DOX treatment demonstrated a decreased number of microvilli an observable deformation, while DOX-Ar-CC-NPs treatment confirmed a relatively polished surface with microvilli disappearance. Additionally, the treatment groups were characterized by membrane blebbing's, cell shrinkage and growth of apoptotic bodies. DNA fragments produced are termed as apoptotic bodies, suggesting that it is in a late period of apoptosis. These results deliver more evidence that DOX-Ar-CC-NPs can induce apoptosis in MCF-7 cells.

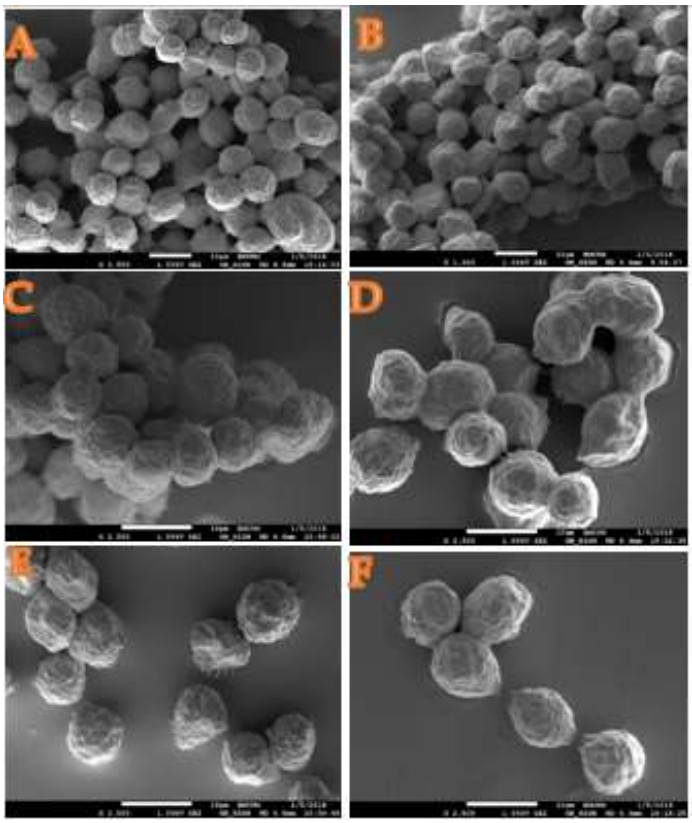

Figure 4: SEM micrographs of surface ultrastructural characteristics of untreated MCF-7 Cells (A and B) control cells demonstrated microvilli magnification (× 2500) and (D, E, and F), Cells Treated with Dox revealing membrane blebbing's, cells shrinkage and also showing apoptotic body both (C and D)/(E, and F) magnification (× 25000) , bar 10 µm.

Ultrastructural Observation of MCF-7 cells using TEM

The micrographs of the control cells and Ar-CC-NPs revealed well dispersed chromatin, clear nuclear membrane in addition to the loss of integrity of cell organelles (Figure 5A and B). The physical ultrastructural characteristics was visibly altered after DOX or DOX-Ar-CC-NPs treatment, demonstrating distinctive apoptotic phenomena (Figure 5C). The major characteristic indication of early apoptosis, which was detected in both

treatment groups were chromatin condensation, cell shrinkage and margination. A great number of vesicles precast in the cytoplasm, while a small number of vacuoles containing DOX-Ar-CC-NPs coacervates were found (Figure 5D). As such, these confirm that DOX-Ar-CC-NPs may have the capacity to internalize into the cells. Similarly, the characteristic of apoptosis, membrane blabbing and apoptotic bodies were detected as shown in Figure 6, which suggests that DOX can increased the percentage of apoptotic cells, compared to the control ($p>0.05$).

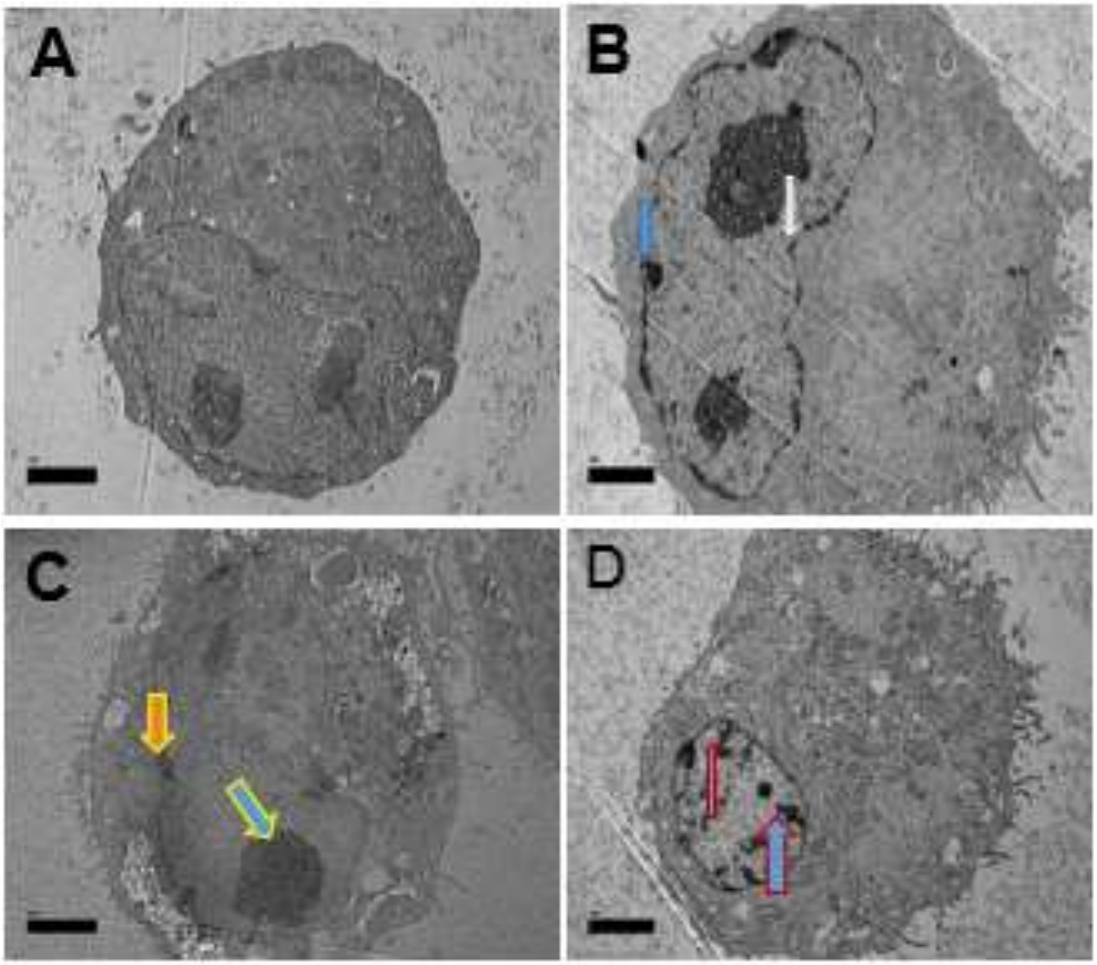

Figure 5. TEM micrographs of ultrastructural features of untreated MCF-7 cells (A), control cells and (B), Treated with NPs revealing normal cellular technique containing unabridged integrity of cells organelle and showing rounded shape cell with nucleus and nucleolus chromatin. Image magnification × 15000, bar 2 μm Ultrastructural alterations of treated MCF-7 cells with Dox alone (C), demonstrated characteristics of early

apoptosis cell shrinkage and chromatin condensation as well as late apoptosis, nuclear collapse, progressing blebbing's , apoptotic body formation and (D), revealed chromatin condensation which are early features of apoptosis

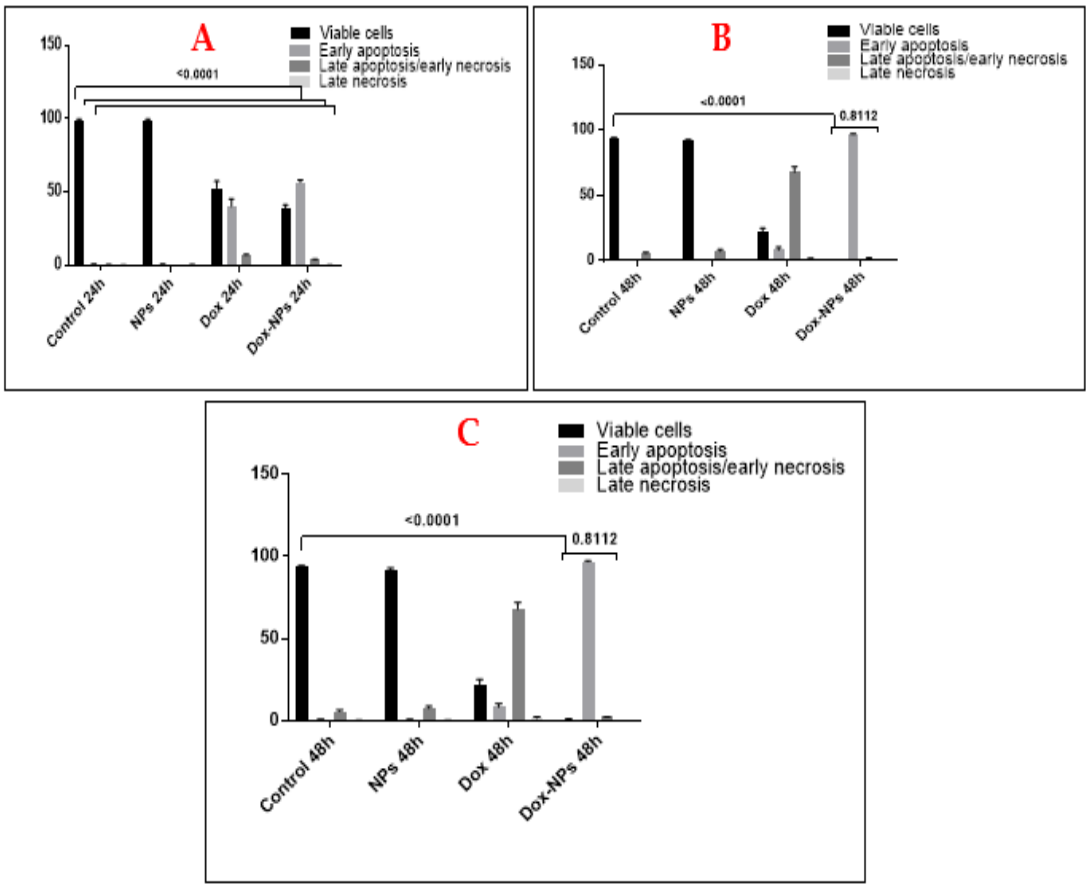

Figure 6: Annexin V assay of MCF-7 cells treated with DOX-r-CC-NPs for 24, 48 and 72 hours. In all sections, the different categories of cell population are represented as, LL (viable cell), LR (early apoptosis), UR (late apoptosis) and UL (necrosis).

In the DOX-Ar-CC-NPs treatment group, the percentages of early apoptotic cells at 24, 48 and 72 hours were 56.69 ± 1.67 %, 96.91± 0.36% and 50.03 ± 0.46%, respectively (Figure 6) Whereas the percentage of late apoptotic cells at 24, 48 and 72 hours were 3.98 ± 0.30%, 2.22 ± 0.24 and 40.34 ± 0.01%, respectively (Figure 6). Additionally, DOX-Ar-CC-NPs treatment considerably increased the percentage of apoptotic cells, compared to the control ($p>0.05$). A similar trend was also detected in the DOX treatment

group. Nevertheless, there were no significant differences between the free NPs group and the control group ($p>0.05$). In all, both DOX and DOX-NPs showed to induce apoptosis of MCF-7 cells in a time-dependent manner.

Quantification of MCF-7 Apoptotic Cell Death using Annexin V and PI Binding Assay table

The MCF-7 display a dot plot in the lower right, as well as upper right quadrant population, imply early and late apoptotic cells in that order while the lower left quadrant denotes viable cells. Upper left quadrant population of cells stained merely with PI denotes necrotic cells. Control was set as cells without any drug treatment. For the control group, the percentage of viable cells after 24, 48 and 72 hours were $98.46 \pm 0.18\%$ and $93.38 \pm 0.92\%$ respectively (Table 1) Whereas the Ar-CC-NPs free group exhibited a percentage of viable cells $98.54 \pm 0.04\%$, $91.63 \pm 1.25\%$ and $92.86 \pm 0.65\%$ after 24,48, and 72 hours, respectively (Table 1). There were no significant different amongst the Ar-CC-NPs group alone and the control group ($P>0.05$), which showed that the Ar-CC-NPs can be presented as influence chemo-resistivity and drug target delivery towards limiting undesirable side effects compared with control groups and Ar-CC-NPs, the percentages of both early apoptosis as well as late apoptosis in DOX and DOX-Ar-CC-NPs groups as significantly increased. Additionally, in the DOX-Ar-CC-NPs treatment group, the percentages of early apoptotic cells after 24, 48 and 72 hours were $93.98\pm 3.48\%$, $36.62\pm 0.24\%$ and $36.60\pm 0.59\%$, respectively (Figure 6). Even though the respective percentages of late apoptotic cells after 24, 48 and 72 hours were $2.65\pm 0.72\%$, $63.23\pm 0.25\%$ and $53.53\pm 0.75\%$, Comparing to the control ($p<0.05$), treatment with DOX-Ar-CC-NPs significantly increased the percentage of apoptotic cells. Similar trends were detected in DOX treatment group. As soon as the cells were treated with DOX at 24, 48 and 72 hours, the average proportion of Annexin V-staining positive cells (number of apoptotic cells) significantly increased from 48.89 to 86.55 and 96.95%, respectively. These results suggest that DOX-Ar-CC-NPs could induce apoptosis of MCF-7 cells in a time –dependent manner.

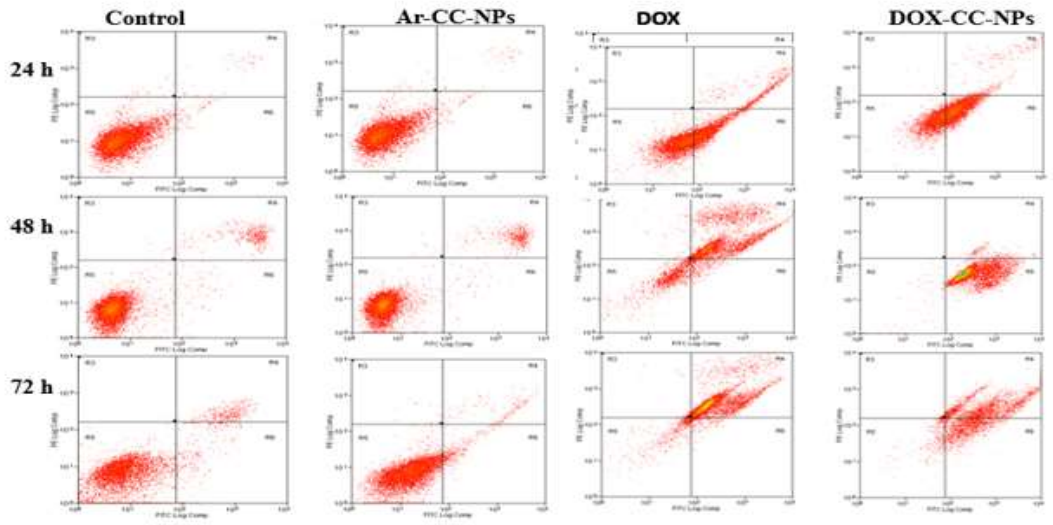

Table 1. Annexin V/ PI apoptosis flow cytometry analysis of MCF7 cells for 24, 48 and 72h after treatment with different groups.

SOD activity

The superoxide dismutase (SOD) activity assay was monitored while some alteration was observed in the MCF-7 cell (Figure), SOD activity was not statistically significant in both treatment groups. The data shows that SOD activity was reduced in MCF-7 cells treatment at IC_{50} concentration (5 % and 13 % relative to controls) for 72 hrs. However, this reduction was not statistically significant.

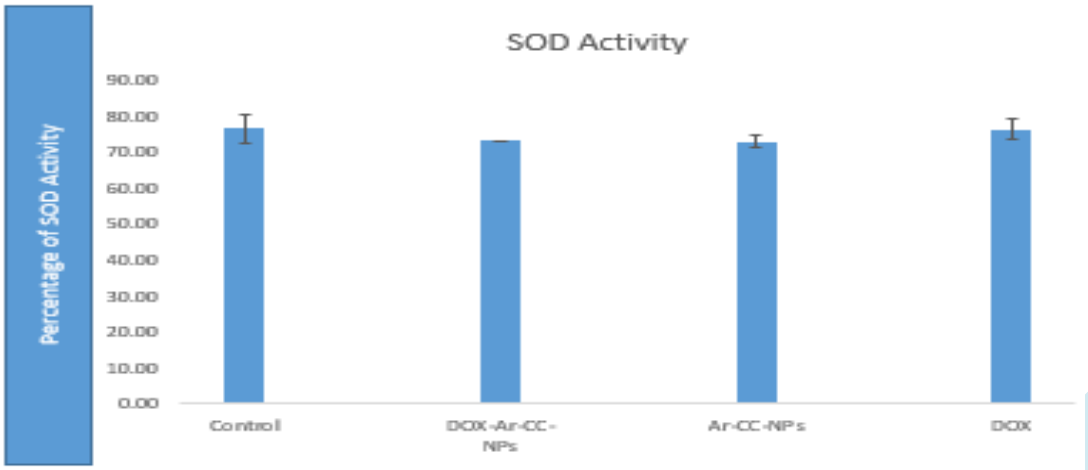

Figure 7. The effect of DOX, DOX-NPs and NPs on SOD activity in MCF-7 cells line. Cells were cultured at IC_{50} concentration doses for 72 hours.

Discussion

Despite the physiological variations in humans, *in vitro* studies are considered the most valuable tool in the development of therapeutic drugs. *In vitro* analyses can enhance the safety and efficacy of novel compounds. Consequently, *in vitro*, techniques are increasingly used to characterize the structural and physicochemical properties of test compounds, including their toxicity (Wilk-zasadna *et al.*, 2014). Appraisal of cytotoxicity of Aragonite Calcium Carbonate nanoparticles is a critical step to take before its biomedical therapeutic applications. This study aimed to determine the apoptotic sound effects, and cytotoxic effects of Doxorubicin conjugated Aragonite $CaCO_3$ nanoparticles (DOX-Ar-CC-NPs) on breast cancer cell-line and its potential mechanism of action. DOX-Ar-CC-NPs significantly reduced cell growth in a concentration and time-dependent manner. It is noteworthy to mention that cell metabolism could differ between cells and DOX-Ar-CC-NPs could activate the apoptotic pathways in cells that are more susceptible to its nontoxic Ar-CC-NPs component. Also, Ar-CC-NPs could affect different components of the apoptotic pathway, and oxidative stress pathways which are much are a risk. These findings showed that DOX-Ar-CC-NPs exhibit selective inhibitory effects against cancer cells without affecting normal cells. This suggests that DOX-Ar-CC-NPs could be a potential chemopreventive agent, ideally for surveillance and targeting breast. Specific targeting of cancer cells increases the therapeutic efficacy of DOX, while reducing off targeted organ effect/side effects (Brannon *et al.,* 2012; Brigger *et al.,* 2012; Ou *et al.,* 2018). The amounts of cell death after treatment were increased, which is illustrated through morphological observations. The microscopic observations revealed that the morphological changes during cell death were consistent with cell apoptosis characteristics. DOX-Ar-CC-NPs effectively induced early apoptosis as evidenced by Acridine Orange (AO) and Propidium Iodide (PI) after 24 and 48 hours and late apoptosis Acridine Orange (AO) and Propidium Iodide (PI) after 72 hours of treatment. On the other hand, MCF-7 cells exhibited late apoptotic breast cancer cells at 48 and 72 hour. Necrotic Acridine Orange (AO) and Propidium Iodide (PI) breast cancer cell populations appeared infrequently. Early apoptotic breast cancer cells attract phagocytes by the release of orange (specific) signals, free of

improvement of inflammation, although late apoptotic and necrotic cells release additional pro-inflammatory threat signals (21). Interestingly, only a few necrotic cells were noticed at 72 hours of treatment. These suggest that the rate of cell death may be affected by the depletion of nutrients in the growth media. Furthermore, flow cytometry analysis revealed that Annexin V, a membrane-associated protein which has a high affinity for Phosphatidylserine (PS) (22) and a flow cytometry analysis exhibited a decline of viable cells percentage with the increasing time of DOX-Ar-CC-NPs for 24 and 48 hours resulted in more percentage of early apoptotic cells, while the treatment over an extended time 72 hours resulted in more cells present in the late apoptosis stage than early apoptosis. Once the plasma membrane becomes permeable, early apoptotic cancer cells transform into late apoptotic cells (23). DOX-Ar-CC-NPs is capable of activating several regulatory mechanisms, resulting in either apoptosis or cell death. When DOX is used alone, weak fluorescence may be observed within the nucleus after 24 hours of incubation followed by centrifugation. In such conditions, it is normal to have a low intracellular concentration of DOX at equilibrium when extracellular DOX is removed.

In this study, the effects of DOX-Ar-CC-NPs and DOX alone in intracellular reactive oxygen species (ROS) were elucidated. Oxidative stress is a key determinant of toxicity mechanisms associated with DOX and nanoparticles (24–26). The interaction between DOX-Ar-CC-NPs and breast cancer cells can induce oxidative stress through ROS production beyond the cellular antioxidant capacity (14,27) Oxidative stress plays a crucial role in a variety of normal biochemical functioning's, and abnormality in its function results in pathological processes. Generally, excessive production of ROS in MCF-7 cell is known to induce apoptosis (28)(29). ROS generation has shown to play an important role in induction apoptosis by treating with encapsulated and free DOX free are reported in the works of Zeng *et al.,* (2015); Pawar *et al.*, (2017). Altogether, the current findings indicate that MCF-7 cell death is determined by ROS production. Hence, cellular redox status may be altered in such a case, resulting in cell death. Besides this, previous research on DOX-Ar-CC-NPs reported that the formulation has high potency towards drug delivery (6,7,11,31).

Conclusion

The synthesized Ar-CC-NPs loaded with DOX is an effective combatant against MCF-7 breast cancer. Its synthesis from novel biomolecules from readily available natural sea water cockle shells gives it excellent nanocarrier qualities which in turn enable its ability to optimize the efficacy of DOX as an anticancer agent. Results of this current study clearly showed that DOX-Ar-CC-NPs is able to induce apoptosis in MCF-7 cells. Thus, demonstrating the high potency of Ar-CC-NPs in drug delivery. More so, cellular uptake analysis and fluorescence microscopy exhibited co-localization of DOX-Ar-CC-NPs within endosomes and lysosomes after labelling. This further stressed the ability of DOX-Ar-CC-NPs induce apoptosis in MCF-7 cells *in vitro*. The quantitative estimation of apoptotic induction capability of DOX-Ar-CC-NPs using Annexin V/PI apoptosis flow cytometry analysis revealed a time-dependent significant increase in the percentage of apoptotic cells. Furthermore, flow cytometry analysis revealed that DOX-Ar-CC-NPs induced apoptosis in MCF-7 cells.

Acknowledgements

Our data were achieved with the assistance Laboratory staff of the Biochemistry Unit, Faculty of Veterinary Medicine Universiti Putra Malaysia. The authors thank the staff of parasitology, Pharmacology & Microscopy unit and, Institute of Bioscience for their help during the study.

Disclosure statement

The authors assert that they have no conflicting interests.

References

1. Jolla L, Kingdom U. Early Redistribution of Plasma Membrane Phosphatidylserine Is a General Feature of Apoptosis Regardless of the Initiating Stimulus : Inhibition by Overexpression of Bcl-2 and Abl. 1995;182(November).
2. Pawar VK, Singh Y, Sharma K, Shrivastav A, Sharma A, Singh A. Doxorubicin Hydrochloride Loaded Zymosan-Polyethylenimine Biopolymeric Nanoparticles for Dual ' Chemoimmunotherapeutic ' Intervention in Breast Cancer. 2017;1857–71.
3. Maruyama N, Nishihara K, Nakasone T, Saio M, Maruyama T, Tedokon I, et al. Triple primary malignancies of surface osteosarcoma of jaw , myelodysplastic

syndrome and colorectal cancer as a second primary cancer detected by PET2 -[18 F]- fluoro - 2 - deoxy - D - glucose positron emission tomography : A case report. 2018;9901–7.

4. Shafei A, El-bakly W, Sobhy A, Wagdy O, Reda A, Aboelenin O, et al. Biomedicine & Pharmacotherapy A review on the e ffi cacy and toxicity of di ff erent doxorubicin nanoparticles for targeted therapy in metastatic breast cancer. Biomed Pharmacother [Internet]. 2017;95(June):1209–18. Available from: http://dx.doi.org/10.1016/j.biopha.2017.09.059
5. Gottesman MM, Fojo T, Bates SE. MULTIDRUG RESISTANCE IN CANCER : ROLE OF ATP-DEPENDENT TRANSPORTERS. 2002;2(January):48–58.
6. Hammadi NI, Abba Y, Noor M, Hezmee M, Shameha I, Razak A, et al. Formulation of a Sustained Release Docetaxel Loaded Cockle Shell-Derived Calcium Carbonate Nanoparticles against Breast Cancer. 2017;1193–203.
7. Fu W, Hezmee M, Noor M, Yusof LM, Ibrahim AT, Keong YS, et al. In vitro evaluation of a novel pH sensitive drug delivery system based cockle shell-derived aragonite nanoparticles against osteosarcoma. 2017;8080(February).
8. Pham VVH, Zhang J, Liu L, Truong B, Xu T, Nguyen TT, et al. Identifying miRNA-mRNA regulatory relationships in breast cancer with invariant causal prediction. 2019;1–12.
9. Wang Z, Deng X, Ding J, Zhou W, Zheng X, Tang G. Mechanisms of drug release in pH-sensitive micelles for tumour targeted drug delivery system : A review. Int J Pharm [Internet]. 2018;535(1–2):253–60. Available from: https://doi.org/10.1016/j.ijpharm.2017.11.003
10. Danmaigoro A, Selvarajah GT, Hezmee M, Noor M, Mahmud R, Abu Z, et al. Development of Cockleshell (Anadara granosa) Derived CaCO 3 Nanoparticle for Doxorubicin Delivery. 2017;
11. Mahmood SK, Shameha I, Abdul B, Ibrahim SM, Yusof LM, Abubakar AA. In Vivo Evaluation of The Novel Nanocomposite Porous 3D Scaffold in a Rabbit Model. 2018;11(May).
12. Hassan S, Prakash G, Bal A, Saghazadeh S, Shrike Y, Khademhosseini A. Nano Today Evolution and clinical translation of drug delivery nanomaterials. Nano Today [Internet]. 2017;15:91–106. Available from: http://dx.doi.org/10.1016/j.nantod.2017.06.008
13. Kiranda HK, Mahmud R, Abubakar D, Zakaria ZA. Fabrication , Characterization and Cytotoxicity of Spherical-Shaped Conjugated Gold-Cockle Shell Derived Calcium Carbonate Nanoparticles for Biomedical Applications. 2018;1–10.
14. Brenneisen P, Reichert AS. Nanotherapy and Reactive Oxygen Species (ROS) in Cancer : A Novel Perspective. 2018;
15. Qin W, Huang G, Chen Z, Zhang Y. Nanomaterials in targeting cancer stem cells for cancer therapy. Vol. 8, Frontiers in Pharmacology. 2017.
16. Plemel JR, Caprariello A V, Keough MB, Henry TJ, Tsutsui S, Chu TH, et al. Unique

spectral signatures of the nucleic acid dye acridine orange can distinguish cell death by apoptosis and necroptosis. 2017;

17. Wilk-zasadna I, Bernasconi C, Pelkonen O, Coecke S. Biotransformation in vitro : An essential consideration in the quantitative in vitro -to- in vivo extrapolation (QIVIVE) of toxicity data. Toxicology [Internet]. 2014; Available from: http://dx.doi.org/10.1016/j.tox.2014.10.006
18. Ou A, Louis H, Oo O, Bi I, Pi A, Philip M. Nanomedicine & Nanotechnology Utility of Nanomedicine for Cancer Treatment. 2018;9(1):1–6.
19. Brannon-peppas L, Blanchette JO. Nanoparticle and targeted systems for cancer therapy ☆. Adv Drug Deliv Rev [Internet]. 2012;64:206–12. Available from: http://dx.doi.org/10.1016/j.addr.2012.09.033
20. Brigger I, Dubernet C, Couvreur P. Nanoparticles in cancer therapy and diagnosis ☆. Adv Drug Deliv Rev [Internet]. 2012;64:24–36. Available from: http://dx.doi.org/10.1016/j.addr.2012.09.006
21. Lucas M, Stuart LM, Savill J, Lucas M, Stuart LM, Savill J, et al. Apoptotic Cells and Innate Immune Stimuli Combine to Regulate Macrophage Cytokine Secretion. 2018;
22. Kooijmans SAA, Vader P. Nanoscale to tumor cells : a plug-and-play approach †. 2018;2413–26.
23. Azizi M, Ghourchia H, Yazdian F, Bagherifam S. Anti-cancerous effect of albumin coated silver nanoparticles on MDA-MB 231 human breast cancer cell line. 2017;(July 2016):1–19.
24. Deavall DG, Martin EA, Horner JM, Roberts R. Drug-Induced Oxidative Stress and Toxicity. 2012;2012.
25. Farhane Z, Bonnier F, Maher MA, Bryant J, Casey A, Byrne HJ. Differentiating responses of lung cancer cell lines to Doxorubicin exposure : in vitro Raman micro spectroscopy , oxidative stress and bcl-2 protein expression. 2017;165(1):151–65.
26. Nebbia C, Girolami F, Carletti M, Gasco L, Zoccarato I, Giuliano A. In vitro interactions of malachite green and leucomalachite green with hepatic drug-metabolizing enzyme systems in the rainbow trout (Onchorhyncus mykiss). Toxicol Lett [Internet]. 2017;280(May):41–7. Available from: https://doi.org/10.1016/j.toxlet.2017.07.900
27. Prasad S, Gupta SC, Tyagi AK. Reactive oxygen species (ROS) and cancer : Role of antioxidative nutraceuticals. Cancer Lett [Internet]. 2017;387:95–105. Available from: http://dx.doi.org/10.1016/j.canlet.2016.03.042
28. Alshammari GM, Ignacimuthu S, Alshatwi AA. ScienceDirect Epoxy clerodane diterpene inhibits MCF-7 human breast cancer cell growth by regulating the expression of the functional apoptotic genes Cdkn2A , Rb1 , mdm2 and p53. Biomed Pharmacother [Internet]. 2017;87:388–96. Available from: http://dx.doi.org/10.1016/j.biopha.2016.12.091

29. Reboredo-rodríguez P, González-barreiro C, Cancho-grande B, Simal-gándara J, Giampieri F, Forbes-hernández TY, et al. E ff ect of pistachio kernel extracts in MCF-7 breast cancer cells : Inhibition of cell proliferation , induction of ROS production , modulation of glycolysis and of mitochondrial respiration. J Funct Foods [Internet]. 2018;45(February):155–64. Available from: https://doi.org/10.1016/j.jff.2018.03.045
30. Zeng L, Pan Y, Tian Y, Wang X, Ren W, Wang S, et al. Biomaterials Doxorubicin-loaded NaYF 4 : Yb / Tm e TiO 2 inorganic photosensitizers for NIR-triggered photodynamic therapy and enhanced chemotherapy in drug-resistant breast cancers. Biomaterials [Internet]. 2015;57:93–106. Available from: http://dx.doi.org/10.1016/j.biomaterials.2015.04.006
31. Ghaji MS, Abu Z, Zakaria B, Shameha ARI, Noor M, Hezmee M, et al. Novelty to Synthesis Nanoparticles from Cockle Shall via Mechanical Method to Delivery and Controlled Release of Cytarabine. 2017;14(xx):1–9.